Chapter 1
General Introduction

General Introduction

1.1 A Brief Introduction to Nanoparticles

The growing science and technology related to nano regime are current inventive branches of sciences and technology that are developing at a very fast pace.[1,2] Particles with at least one of the dimensions in the range of 1−100 nm, so called nanomaterials, are larger than individual atoms and smaller than the bulk solids.[3] Therefore, particles in the nanometer length scale, exhibit interesting optical, electronic, catalytic, and magnetic properties with varying size, shape/morphology and dispersity that are, surprisingly, different from the corresponding individual atoms and the complement bulk solids.[4-6] With decreasing the size of the particles to nanoscale dimension, the 'surface-to-volume' ratio of the nanoparticles sharply increases and exhibits quantum size effect.[7] Generally, metals have properties which are termed as "metallic properties" that includes conduction of heat and electricity, do not have any band gap between valence band and conduction band, are good conductor of heat and electricity and do not exhibit any characteristic colour in their bulk state. The significant changes in optical and electronic properties with shrinking the sizes of the solids to the nano-dimension are governed by the variation of sizes and shape of the nanostructures. The interesting exhibition of characteristic physicochemical properties of the manganese oxides nanomaterials or their composites in their nanoscale dimension has been of considerable interest in recent times. Nanoparticles of metal oxide demonstrate widely interesting morphology-dependent physicochemical properties which are, further, accelerated by composites with noble metals nanoparticles or with other metal oxides at the nanoscale dimension.

1.1.1 Electronic Properties of Nanoparticles

Nanoparticles are comprised of a large number of atoms or molecules bonded together and may be distributed in gaseous, liquid or in solid substances. The interesting properties of nanoscale materials are depending upon the number of surface atoms and the surface area which are specified as intrinsic size effects and extrinsic size effects. Intrinsic size effects concern specific changes in volume and surface material properties.

Experimentally, they deal with electronic and structural properties, namely, ionization potentials, binding energies, chemical reactivity, crystallographic structure, melting temperatures, and optical properties of metal clusters that depend upon the particle size and geometry.[8] As the particle size increases, the energy levels continue to split and finally, merge into the quasi-continuous band structure in the bulk solid. The splitting patterns in energy level arising due to the discretion (quantization) of electron energy levels, are known as quantum size effects. For small sizes of the particles, the optical properties become size dependent, whereas, for larger ones, the electrodynamic theory can be applied using bulk optical constants, and this is known as extrinsic size effect.Confinement and quantum size effects in nanoparticles induce properties that are significantly different from those of the bulk material as a result of their reduced dimensions.[9] Because of these unique properties, nanomaterials have become a focus of research in modern technology. For example, semiconductor nanoparticles (quantum dots) exhibit discrete energy bands and size-dependent band gap energies; conducting nanoparticles exhibit large optical polarizabilities and nonlinear electrical conductance; and ferromagnetic nanoparticles become superparamagnetic, with size-dependent magnetic susceptibilities.[10-12]

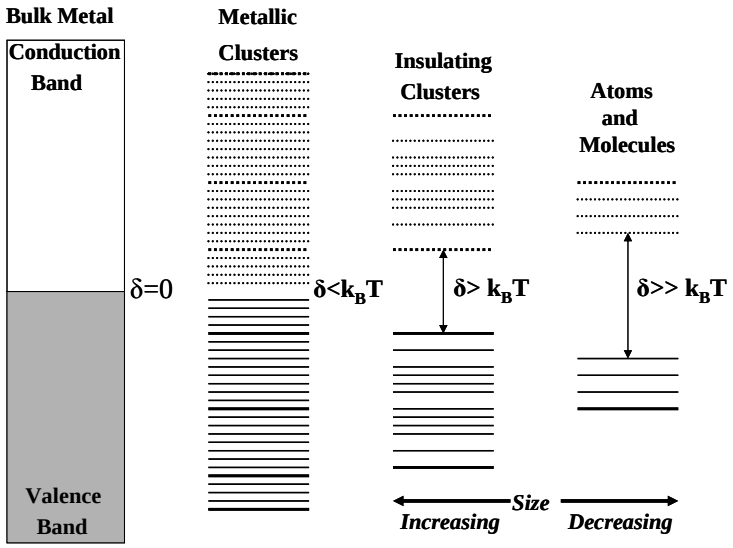

Fig. 1.1. Schematic presentation of the density of states with change in the number of atoms in the system

1.1.2 Surface Activity of the Nanoparticles: High Surface-to-Volume Ratio

In a metal cluster, atoms at surfaces have fewer neighbours than atoms in the bulk. As a result, the atoms in the bulk are co-ordinatively saturated while the atoms on the surface are co-ordinatively unsaturated. Because of this lower coordination and unsatisfied bonds, surface atoms are less stabilised than bulk atoms. The smaller a particle, the larger the fraction of atoms at the surface and the higher the average binding energy per atom. One distinguishing characteristic of nanometer scale structures is that unlike macroscopic materials, they typically have a high percentage of their constituent atoms at the surface. The volume of an object ($V \propto R^3$, where R is the characteristic length) decreases more quickly than its surface area ($S \propto R^2$) as the size diminishes: $S/V \propto R^{-1}$, where, R has atomic or molecular dimensions (Fig.1.2.) This scaling behavior leads, in the most extreme case, to structures where nearly every atom in the structure is interfacial and in some sense, it could be assumed that nanostructures are "all surface". The term 'surface' has been used to indicate the geometrical separation between two or more phases of matter whereas the term 'interface' implies a region of finite thickness over which the phase change occurs.[13]

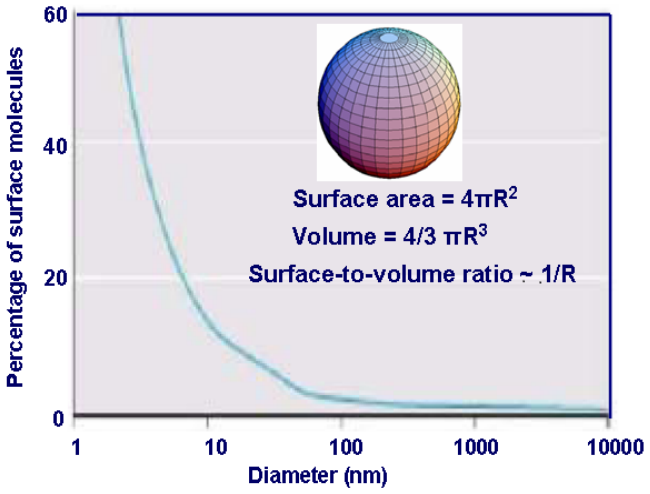

Fig. 1.2. Profile showing the percentage of surface atoms as a function of particle diameter at the nanoscale dimension.

1.2 Family of Manganese Oxides

Manganese is the fifth most abundant metal on the Earth's crust, and the second most common trace metal after iron, found at about 1/50 the abundance of iron. Manganese is distinctive for being able to exist in a great number of oxidation states, from 0 to +7. In nature, however, it is primarily found as Mn(II), Mn(III), and Mn(IV) states. The Mn^{2+} (manganous) cation is the most important soluble form of manganese in nature, though, certain important Mn (II) salts such as manganous carbonate (rhodochrosite) have only low or negligible solubility. The Mn^{3+}

(manganic) ion is unstable in neutral solution unless strongly complexed; it rapidly disproportionates to Mn^{2+} and MnO_2. The ions, Mn (III) and Mn(IV) are generally found as insoluble oxides or hydrous oxides, Mn(IV) most, notably, as MnO_2. These oxides are brown- or black-coloured. Mn(II) oxidation can lead to a variety of oxides, depending on the exact conditions of oxidation; some possibilities are ß-, γ-, and δ-MnO_2, α-, ß-, and γ-MnOOH, Mn_2O_3, Mn_3O_4, and $Mn(OH)_3$.[14] Any oxidation not rigidly controlled is likely to result in a nonstoichiometric mixture of these oxides. Such mixed oxides are often referred to as "MnO_x" for convenience, with *x* ranging from 1.0 to 2.0. Furthermore, some of the oxides are metastable and convert to higher oxides upon aging.[15] An important complication of studying Mn(II) oxidation is that manganese oxides provides binding sites for trace metals, including, Mn^{2+}, and that MnO_x catalyzes oxidation of bound Mn(II).

1.2.1 Manganese Oxides at the Nanoscale Dimension

Natural manganese oxides are generally formed in surficial environments that are near ambient temperature and water-rich, and may be exposed to wet-dry cycles and a variety of adsorbate species that influence dramatically their level of hydration. Manganese oxide minerals are often poorly crystalline, nanophasic and hydrous. In the near-surface environment, they are involved in processes that are important to life, such as, water column oxygen cycling, biomineralization, and transport of minerals/nutrients through soils and water. These processes, often involving transformations among manganese oxide polymorphs, are governed by a complex interplay between thermodynamics and kinetics. Manganese oxides are also used in technology as catalysts, and for other applications. The major goal of this dissertation is to examine the energetics of bulk and nanophase manganese oxide phases as a function of particle size, composition, and surface hydration. Careful synthesis and characterization of manganese oxide phases with different surface areas provided samples for the study of enthalpies of formation by high temperature oxide melt solution calorimetry and of the energetics of water adsorption on their surfaces. These data provide a quantitative picture of phase stability and how it changes at the nanoscale.

Manganese oxide nanomaterials potentially hold great promise for sustainable nanotechnology. In addition to being of high interest for a variety of applications, they are based upon earth abundant elements, as manganese is the twelfth most abundant

element on the planet and the third most common transition element after iron and titanium.[16] Manganese oxides also are generally lower toxicity compounds than other materials upon which nanomaterials are commonly based, such as, various chalcogenides. One of the manganese oxides of interest for multiple technologies and the focus of this study is Mn_3O_4, also known as hausmannite. Mn_3O_4 is a mixed valence oxide that has been a promising candidate for a range of applications, including, catalysis.[17–19] Manganese oxide minerals have been used for thousands of years, such as, by the ancients for pigments and to clarify glass, and today as ores of manganese metal, catalysts, and battery material. More than 30 manganese oxide minerals occur in a wide variety of geological settings. They are major components of Mn nodules that pave huge areas of the ocean floor and bottoms of many fresh-water lakes. Manganese oxide minerals are ubiquitous in soils and sediments and participate in a variety of chemical reactions that affect groundwater and bulk soil composition. Manganese oxides are potent sinks for trace metals, contaminants, and nutrients in the environment.[20] By weathering of igneous and metamorphic rock, Mn (II) is released. This Mn (II) is oxidized to Mn(III) and Mn(IV) in presence of oxygen. A wide range of compounds can form, more than 30 known oxide and hydroxide minerals by manganese. Sometimes, they also appear in combined valence forms, containing both Mn(III) and Mn(IV). Manganese oxides are characterized by open crystal structures, large surface areas and high negative charges.[21] Their typical occurrence as fine-grained mixtures makes it difficult to study their atomic structures and crystal chemistries. In recent years, however, investigations using transmission electron microscopy and powder X-ray and neutron diffraction methods have provided important new insights into the structures and properties of these materials. Basically, manganese oxides are MnO_6 octahedra that can be corner-, edge- or face sharing and thus, forming secondary structures, like, phyllomanganates and tectomanganates. The phyllomanganates consist of layered sheets of edge-sharing MnO_6 octahedra. Between those sheets water or small actions can be stored in exchangeable form. Phyllomanganates exist in two forms, separated by the width of their interlayer: with 7 °A (birnessite, chalcophanite and MnO_2) and 10 °A (lithiophorite or buserite) d-spacings. The structure with 10 °A d-spacing contains an additional layer of water. 10°A manganese oxides collapse to 7°A phyllomanganates when they are protonated or dehydrated.[22]

The crystal structures for todorokite and birnessite, two of the more common manganese oxide minerals in terrestrial deposits and ocean nodules, were determined by using powder x-ray diffraction data and the Rietveld refinement method. Because of the large tunnels in todorokite and related structures there is considerable interest in the use of these materials and synthetic analogues as catalysts and cation exchange agents. Birnessite-group minerals have layer structures and readily undergo oxidation reduction and cation-exchange reactions and play a major role in controlling groundwater chemistry.[23] The improvement pursued in active materials mainly concerns high reversible capacitance, structural flexibility and stability, fast cation diffusion under high charge–discharge rates, and environmental friendliness. As a transition metal element, manganese can exist as a variety of stable oxides (MnO, Mn_2O_3, Mn_3O_4 and MnO_2)[24-26] and crystallise in various types of crystal structures, as shown in Fig. 1.3.

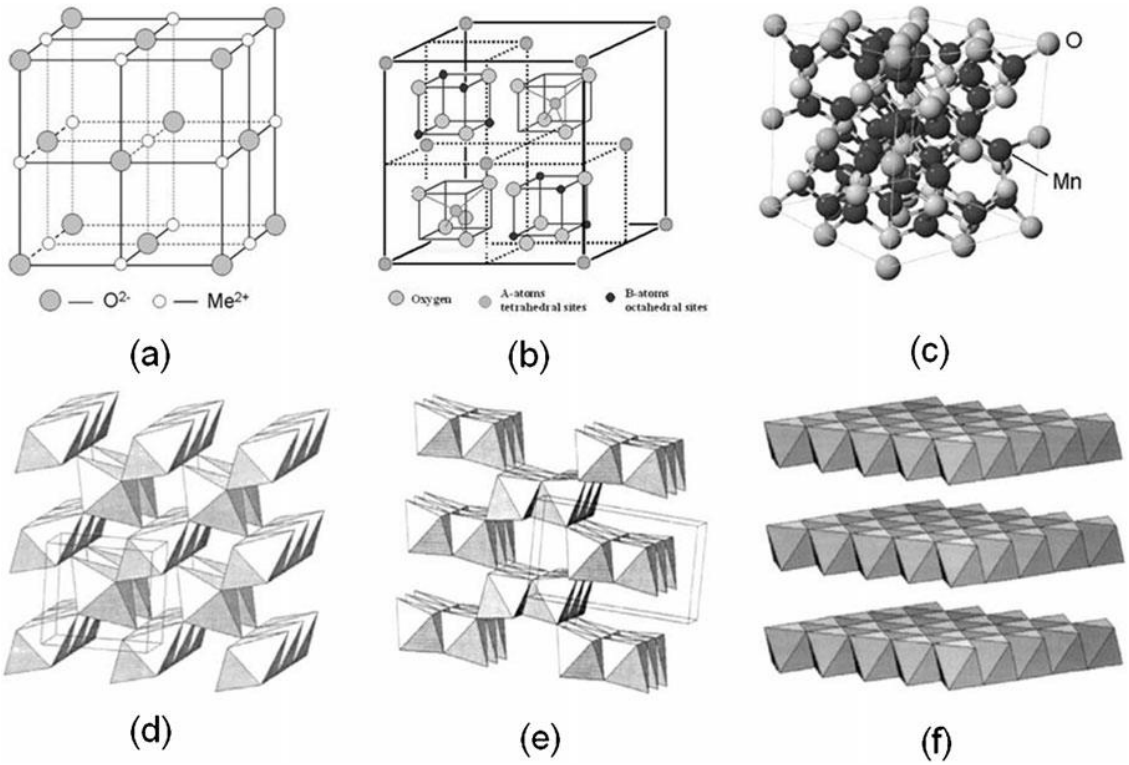

Fig. 1.3. Schematic representation of the crystal structure of manganese oxides. (a) Rock salt; (b) spinel (Mn_3O_4); (c) bixbyite (Mn_2O_3); (d) pyrolusite β-MnO_2 (rutile-type) (note the single chains of edge-sharing octahedra); (e) ramsdellite (diaspore-type) ([MnO_6] octahedra form infinite double layers); (f) phyllomanganate (birnessite–buserite family of layered MnO_2). In this idealized representation there are alternate layers of full and empty octahedral sites. Reproduced from Ref. 27. Copyright (2007) American Chemical Society.

1.2.2. Physicochemical Properties of Manganese Oxide Nanoparticles

Associated with a wide diversity of crystal forms, defect chemistry, morphology, porosity and textures, manganese oxides exhibit a variety of distinct physicochemical properties. These structural parameters play a crucial role in determining and optimizing the physicochemical properties when manganese oxides are applied as catalytic materials. Manganese oxides are materials of considerable importance due to their interesting structural, electronic and magnetic properties that arise from their outstanding structural flexibility combined with novel physical and chemical properties.[28-29] Moreover, manganese oxides are ubiquitous in nature and environmental friendly that deserve their applications in catalysis, renewable energy, and environmental remediation. Among the series of manganese oxides available in various oxidation states of manganese (II, III, IV), Mn_3O_4 (hausmannite) has been found to be an effective and inexpensive catalyst in versatile reactions.[30-36] The corresponding surface energy values of Mn_3O_4 (0.96 ± 0.08 J m^{-2}), Mn_2O_3 (1.29 ± 0.10 J m^{-2}), and MnO_2 (1.64 ± 0.10 J m^{-2}), suggest considerable thermodynamic stability of Mn_3O_4 over other oxidation states.[37] Moreover, Mn_3O_4 possess several special structural attributes due to the followings, (i) it shows semicovalent character in tetrahedral sites (Mn(II) occupancy with Mn–O distance of 1.812 Å) and in the apical bonds of octahedral sites (Mn(III) occupancy with Mn–O lengths of 2.386 Å; (ii) the remaining bonds of the octahedra display ionic character with a Mn–O length of 2.977 Å; and (iii) the observed distortion in the octahedra found in both phases that can be explained by a Jahn–Teller effect due to the d^4 state of the Mn(III) atoms in high spin configuration. Bulk Mn_3O_4 is a p-type semiconductor with a wide direct band gap of 2.3 eV and is the stablest among all the manganese oxides possessing tetragonally distorted spinel structure.[38-40] The size and shape-controlled synthesis of manganese oxides (MnOx) nanomaterials has attracted considerable interest from both academia and industry due to their tuneable physicochemical properties and several applications.[41-44] Investigation of the influence on these characteristics of manganese oxides on capacitor performance is the basis of a rational design of improved electrode materials. Extensive efforts have been dedicated to adjust synthesis conditions to obtain manganese oxides with desirable morphologies, defect chemistry (cation distributions and oxidation states) and crystal structures to improve the subsequent capacitance and power characteristics.[45] Observing biogenic

manganese oxidation, one of the questions is, why bacteria oxidise Mn(II). There are assumptions, that manganese oxidation by bacteria is an accidental occurrence or an evolutionary remainder.[46] But there are also some indications, that bacteria can use manganese oxidation for their benefit. One possibility is, that bacteria use manganese oxidation to derive energy for chemolitho-autotrophic growth. Oxidising Mn(II) to Mn(III) or Mn(IV) is thermodynamically favourable, but there is still no distinct evidence, that bacteria oxidise Mn(II) for ATP generation. Producing storage for an electron acceptor is a more likely option. Thus, an electron acceptor could be stored, until carbon and energy become available again.[47]

Another reason for biogenic manganese oxidation could be the use of manganese in cellular mechanisms. Manganese can be used as an antioxidant, protecting cells from reactive oxygen species (ROS). These are, e. g., the superoxide radical, hydroxyl radical, hydrogen peroxide or singlet oxygen. Certain amount, ROS can be produced by cells as by-products of respiration. With Mn(II) oxidation, bacteria are able to protect themselves, even if they do not posses a superoxide dismutase, which is the option most often used for ROS scavenging. An open question here is, whether the oxidation of Mn(II) is used intracellular or on the innermembrane, because the bacteria seem to precipitate manganese oxides extracellular. It was speculated, that the bacteria use manganese oxidation to protect themselves from oxidants in their environment.[48]

1.2.2.1. Photocatalytic Reactions using Manganese Oxides

Photocatalytic water splitting paves an avenue for solar hydrogen production. Photocatalysis is classified into two categories. One is the application to the improvement of the living environment, such as, anti-stain, self-cleaning, and superhydrophilicity properties. Another direction of photocatalysis is light-energy conversion as represented by water splitting. Water splitting using light energy has been studied for a long time using powder and electrode systems since the Honda-Fujishima effect was reported.[49] The final target of this research field is to achieve an artificial photosynthesis and solar hydrogen production from water. The search for suitable semiconductors as photocatalysts for the splitting of water into hydrogen gas using solar energy is one of the noble missions of materials sciences. The fabrication of metal oxide superstructures has fascinated scientists for studying the physics of materials in two- or three-dimensions and their potential technological

applications.[50,51] Self-organisation of metal oxide nanostructures provides extraordinary richness of morphological and physicochemical diversity for emerging unprecedented architectures.[52] Manganese oxides are materials of considerable importance due to their interesting structural, electronic and magnetic properties that arise from their outstanding structural flexibility combined with novel physical and chemical properties.[53-55] The removal of the non-biodegradable organic chemicals is a global ecological problem. Dyes are an important class of synthetic organic compounds which are commonly used in textile industries and therefore, are common industrial pollutants. However, due to the inherent stability of modern dyes, conventional biological treatment methods for industrial waste water are ineffective. Photocatalysis, where photons are used for catalytically activating chemical reactions on the surface of photosensitized catalysts, remains one of the leading hubs of research for harvesting the solar light.[56]

1.2.2.2. Selective Oxidation of Organic Molecules using Manganese Oxides as Catalysts

In recent years, size and shape-controlled synthesis of manganese oxides (MnO_x) nanomaterials has fascinated considerable interest from both academia and industry due to their tuneable physicochemical properties.[57-59] Manganese oxides are the most attractive inorganic materials owing to their structural flexibility and availability of different oxidation states of manganese (II, III, IV) that have envisaged their structural, transport and magnetic properties in a diverse range of niche applications.[60] Among the different oxidation states of manganese oxides, Mn_2O_3 is well known as cheap and environment-friendly catalyst and could be employed as ideal candidate for the removal of CO and NO_x from waste gas,[61] decomposition of H_2O_2 into hydroxyl radicals in the catalytic peroxidation of organic effluents and as an oxygen storage component. While the catalytic activity of these materials at the nanoscale dimension depends strongly on their surface properties, the reactivity and selectivity of nanoparticles can be tuned through controlling the morphology because the exposed surfaces of the particles have distinct crystallographic planes depending on their shape.[62] Therefore, synthesis of Mn_2O_3 nanoparticles with well-controlled morphology and a narrow size distribution is desirable for achieving practical applications, such as, catalysis. Mn_2O_3 is generally considered to be the most favorable manganese oxide, while MnO_2 only shows moderate activity.[63,64]

1.2.2.3. Electrocatalytic Reactions using Manganese Oxides

Manganese oxide-based electrodes, either fabricated as a single nanostructured component with desirable physicochemical features or assembled with conductive polymers and porous carbon architectures, open new possibilities for the development of advanced ECs. The strategies can be generalized as the following options: (i) chemical and structural modification of manganese oxide materials to introduce more electrochemically active sites for the redox reaction between the Mn(III) and Mn(IV), (ii) shortening of the transport path length for both electrons and cations by using porous, high surface area, and electronically conducting carbon architectures and (iii) addressing of the low structural stability and flexibility and electrochemical dissolution of active materials through application of conductive polymers in manganese oxide materials. There are some reviews that cover different topics in the development of electrocatalysts.[65-67]

In natural photosynthesis, and many protocols designed for artificial photosynthesis, water oxidation, $2H_2O \rightarrow 4H^+ + O_2 + 4e^-$, is a significant step.[68-69] Plant life is based on settled complex catalytic systems for the disintegration of water into its elements, and our understanding of these systems is pointing the way to the design of simpler catalysts. The oxidation of H_2O to O_2 is the key challenge in the production of chemical fuels from electricity.[70-71] Although, several types of catalysts have been developed for this reaction, ample challenges remain towards the eventual goal of an efficient, inexpensive and robust electrocatalysts. Particularly, nanometer-sized manganese oxides are of great significance in that their large specific surface areas and small sizes may bring some novel electrical, magnetic, and catalytic properties different from that of bulk materials. The shape, size and composition of metal oxide nanoparticles are the key parameters in determining their electrocatalytic performance.[72] Water oxidation has become a very active area of research in recent years, inspired by energy challenges and by the incipient understanding of photosystem II.[73] Designing a bimetallic catalyst composed of nickel and manganese oxide is based on the premise that the incorporation of multivalent manganese in the bimetallic oxide and/or redox characteristics of manganese oxide could potentially downshift the onset potential/reduce the activation energy of nickel oxyhydroxide formation and thereby, facilitate urea oxidation at lower overpotentials.[74]

Metallic platinum and oxides/hydroxides of iridium, ruthenium, nickel and other metals have long been used as anodes for this reaction,[75] and recent discoveries of cobalt/phosphate and related catalysts have generated much interest because of their low cost.[76] Amongst the transition metal electrocatalysts, manganese-based systems are of significant interest because of the large scale earth-abundance of manganese minerals as well as these materials mimic the role of manganese in biological water oxidation reaction in the process of Photosystem II.[77-80] A closer inspection in the series of manganese oxides available in various oxidation states of manganese (II, III, IV), hausmannite (Mn_3O_4) has been found to be an efficient and inexpensive catalyst in a number of oxidation and reduction reactions.[81] The synthesis of nanocomposites containing two or more disparate functionalities have been of significant interest due to their altered and/or enhanced physicochemical properties.[82-83] Even though significant amount of work has been performed on water-oxidation catalysis, many fundamental questions and practical challenges remain, and improvements are needed in cost, durability and overpotential. However, the synthesis of nanocomposites containing two or more disparate functionalities has been of significant interest due to their altered and/or enhanced physicochemical properties. Therefore, to investigate the integration of manganese oxides with other components is of significant interest.[84]

1.2.2.4. Synthesis of Metal Oxide Nanocomposites for Sensory Application

Mixed metal oxide systems used in sensing applications can be classified into three groups. First category involves chemical compounds resulting from the chemical interaction between various oxides, like, $ZnSnO_3$ and Zn_2SnO_4 compounds formed in the ZnO-SnO_2 system[85] and the crystal $CdIn_2O_4$ which is an effective sensor for CO, produced by the interaction of CdO with In_2O_3.[86] The phase α-$SnWO_4$, sensitive to small amounts of CO and NO, was observed in the system SnO_2-WO_3.[87] The second category, includes, mixed oxides, which can form solid solutions. An example of such a system is the mixture of TiO_2 and SnO_2, which form solid solutions over the entire range of compositions but only above a certain critical temperature.[88] The third group consists of systems that give neither individual compounds nor solid solutions. These systems contain mixtures of metal oxide nanocrystals interacting with each other, such as, mesostructured manganese oxide/gold, Au-Mn_3O_4, Au-ZnO, In_2O_3-SnO_2, TiO_2-WO_3 and many others, in fact, only mixed metal oxides of the third group can be regarded as composite materials.[89-91]

1.2.2.4.1. Sensory Mechanism

Conductivity, largely, determines the sensory phenomena observed in nanocrystalline SnO_2 + In_2O_3 films. The effect of composition on sensory characteristics of such films had been investigated for the detection of hydrogen and carbon monoxide. The temperature dependence of the sensitivity S (S = R_o/R, where, R_o and R are the sensor resistances in pure air and in air containing analysed gas, respectively) has been shown to be typical for such sensors, and characterised by a maximum (S_{max}) at a certain temperature (T_{max}).

1.2.1.4.2. Gas Sensing Devices

The sensor response (S), for a particular VOCs, is calculated using the relation,

$$S(\%) = \frac{(R_{voc} - R_{air})}{R_{air}} \times 100 \qquad (1.1)$$

where, R_{voc} is the resistance of the material in presence of VOCs gas and R_{air} is the film resistance in presence of dry air. Considering the influence factors on gas sensing properties of metal oxides, it is necessary to reveal the sensing mechanism of metal oxide gas sensor. The exact fundamental mechanisms that cause a gas response are still controversial, but essentially trapping of electrons at adsorbed molecules and

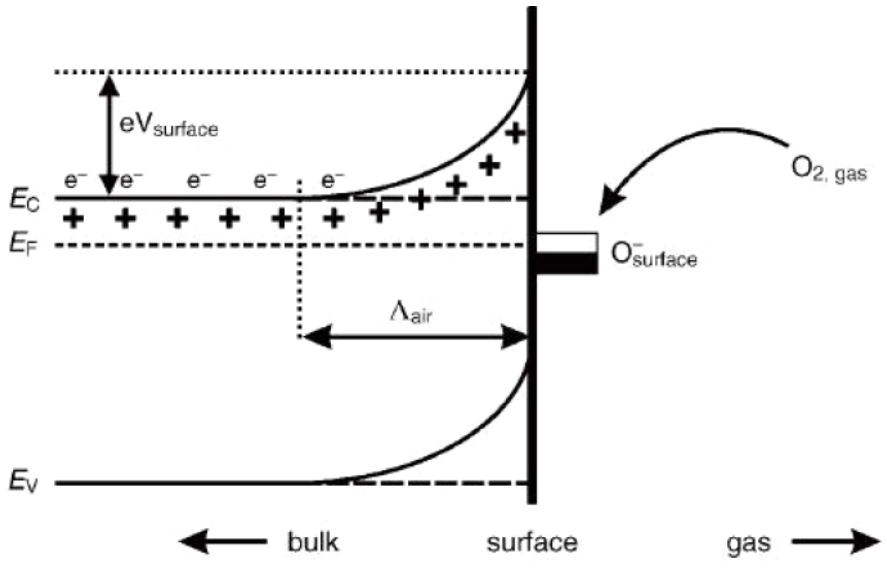

Fig. 1.4 Schematic diagram of band bending after chemisorptions of charged species (here the ionosorption of oxygen) EC, EV, and EF denote the energy of the conduction band, valence band, and the Fermi level, respectively, while Λair denotes the thickness of the space-charge layer, and eV surface denotes the potential barrier. The conducting electrons are represented by e– and + represents the donor sites. Reproduced from Ref. 90. Copyright (2006) Wiley-VCH.

band bending induced by these charged molecules are responsible for a change in conductivity. The negative charge trapped in these oxygen species causes an upward band bending and thus a reduced conductivity compared to the flat band situation.[90] As shown in Fig.1.4 when O_2 molecules are adsorbed on the surface of metal oxides, they would extract electrons from the conduction band E_c and trap the electrons at the surface in the form of ions. This will lead a band bending and an electron depleted region. The electron-depleted region is so called space-charge layer, of which thickness is the length of band bending region. Reaction of these oxygen species with reducing gases or a competitive adsorption and replacement of the adsorbed oxygen by other molecules decreases and can reverse the band bending, resulting in an increased conductivity. O^- is believed to be dominant at the operating temperature of 300–450 °C.

1.2.1.4.3. Sensing Operating Temperature

The operating temperature is one of the important parameters that determine the sensitivity of the ceramic gas sensor. The response (resistance value change) to the presence of a given gas depends on activation processes *viz.* the speed of chemical reaction on the surface of the grain and speed of the diffusion of the gas molecule to the surface. The activation energy of the chemical reaction is higher. At low temperatures, the response is controlled by the speed of chemical reaction and at high temperatures, it is restricted by the speed of diffusion of gas molecules. At intermediate temperatures, the speed of the two processes becomes equal. At this temperature, the response is highest. The sensitivity of most of the sensors presents a trend of increase-maximum-decay to various gases with increase in temperature.

1.2.1.4.4. Sensor Resistance to Gas Concentration

This characteristic explains influence of gas concentration (C_g) on sensor resistance (R_s) or conductivity (G_s). At low concentration of the gas in air atmosphere, at fixed constant temperature, the conductivity (G_s) is given by

$$G_s = K.C_g^{\alpha}$$

Where, K and α are constants, and C_g stands for gas concentration parameter in air.

1.2.1.4.5. Sensitivity

The sensitivity is a degree of the influence of a certain gas on the resistance of a sensor. It is generally determined by the ratio R_a of the resistance in the air to the resistance R_g in a gas with given concentration

$$S_g(\%) = \frac{R_a}{R_g} \text{ X } 100$$

It is a function of concentration of gas and nature of sensing material. In an oxidizing gas medium, the resistance of sensor rises and decreases in a reducing gas atmosphere. Hence, for the oxidising gases, $S_g < 1$ and for reducing gases, $S_g > 1$.

1.2.1.4.6. Selectivity

Selectivity is the capability of a sensor to respond to particular gas in the presence of other gases. It is closely connected with operating temperature. The sensor reactions to the influence of a gas atmosphere containing gases of various chemical compositions can be expressed as superposition of the effects of all of the gases present. The sensor must therefore be selective, i. e., it must respond to one particular gas only. The process of detection of gases is related to the adsorption of gas molecules on the surface of the grains. The adsorption is accompanied by a chemical reaction occurring on the surface. The chemical reaction is characterized by activation energy which demands increased temperature for effectiveness of the sensor. The sensitivity, selectivity, and operating temperature are interrelated and solve simultaneously.[92]

1.2.2.5. Magnetic Properties of Manganese Oxides Nanoparticles

Metal oxide nanocrystals are expected to find useful applications in catalysis, energy storage, magnetic data storage, sensors, and ferrofluids [93] In particular, colloidal metal oxide nanocrystals are of great interest for technological applications owing to their unique size-dependent properties and excellent processability. Manganese oxides are widely used as electrode materials,[94] catalysts,[95] and soft magnetic materials[96] It has been reported that Mn_3O_4 nanoparticles show ferromagnetic behaviors at low temperatures, whereas, they were paramagnetic at room temperature.[97,98] However, MnO nanoparticles (5–10 nm in diameter) show weak ferromagnetic behavior at low temperatures, although bulk MnO shows antiferromagnetic behavior with T_N~125 K.

The observed weak ferromagnetism has been ascribed to the presence of noncompensated surface spins on the antiferromagnetic core of the MnO nanoparticles.[99] Measurements of size-dependent magnetism, however, have never been reported for MnO nanoparticles. Very often, MnO nanomaterials showed the expected weak ferromagnetic behavior at low temperatures, but unusual size-dependency of magnetic properties was observed for MnO nanoparticles.[100]

Manganese oxide (MnO_2) is a material of long-standing interest for electrochemical energy storage, starting with its use in zinc carbon Laclanche cells in the 1860s. Lee and Goodenough[101] discovered the application of MnO_2 to aqueous-based ultracapacitors in 1999. In some important articles, hollow manganese oxide nanoparticles (HMON), prepared by a bio-inspired surface functionalization approach, have, subsequently, functionalized with a therapeutic monoclonal antibody, Herceptin, to selectively target cancer cells. Confocal microscopy and magnetic resonance imaging studies revealed that the surface functionalised HMON enabled the targeted detection of cancer cells in T1-weighted MRI as well as the efficient intracellular delivery of *si*RNA for cell-specific gene silencing. These nanomaterials are expected to be widely exploited as multifunctional delivery vehicles for cancer therapy and imaging applications.[102] Chang and his group have reported hierarchical MnO_2-coated magnetic nanocomposite (Fe_3O_4/MnO_2), synthesised by a mild hydrothermal process and its application for removing heavy metal ions from contaminated water systems.[103] One important example is the electrically conductive manganese oxide, which stores electrical charge by a double insertion of electrons and cations into the solid state.[104]

1.3 Conclusion

Manganese is very important earth-abundant element in the periodic table. Due to capability of large number of oxidation states (from 0-VII), manganese can form several important oxides with huge applicability. All these oxides can be synthesized in the nanometer regime. Which motivate us to do research-work with manganese oxides in the nano/micrometre region, and notice on their several physico-chemical properties and finally application of the synthesized materials in the fields like catalysis, photocatalysis, electrocatalysis and sensing technology depends on feasibility of the materials.

1.4 References

1. J. A. Schuller, E. S. Barnard, W. Cai, Y. C. Jun, J. S. White and M. L. Brongersma, *Nat. Mater.*, 2010, **9**, 193-204.
2. L. C. Kennedy, L. R. Bickford, N. A. Lewinski, A. J. Coughlin, Y. Hu, E. S. Day, J. L. West and R. A. Drezek, *Small*, 2010, **7**,169-183.
3. D. J. Irvine, M. C. Hanson, K. Rakhra and T. Tokatlian**,** *Chem. Rev.*, 2015**, 115**, 11109–11146.
4. V. Giannini, A. I. Fernández-Domínguez, S. C. Heck, and S. A. Maier, *Chem. Rev.*, 2011, **111**, 3888–3912.
5. A. B. Chinen, C. M. Guan, J. R. Ferrer, S. N. Barnaby, T. J. Merkel and C. A. Mirkin, *Chem. Rev.*, 2015, **115**, 10530–10574.
6. K. M. Mayer and J. H. Hafner, *Chem. Rev.*, 2011, **111**, 3828–3857
7. S. M. Morton, D. W. Silverstein and L. Jensen, *Chem. Rev.*, 2011, **111**, 3962–3994.
8. S. K. Ghosh, and T. Pal, *Chem. Rev*., 2007, **107**, 4797–4862.
9. K. V. P. M. Shafi, A. Ulman, A. X. Yan, N. -L. Yang, C. Estournes, H. White and M. Rafailovich, *Langmuir*, 2001, **17**, 5093.
10. L. E. Brus, .*J. Mater. Res*., 1989, **4**, 104
11. H. Sakaki and H. Noge, In *Nanostructures and Quantum Effects*; Springer-Verlag: Berlin, 1997.
12. U. Woggon, In *Optical Properties of Semiconductor Quantum*; Springer-Verlag: Berlin, 1997.
13. M. El-Sayed, *Int. Rev. Phys. Chem.*, 2000, **19**, 409-453.
14. W. Stumm and J. J. Morqan, In *Aquatic Chemistry An Introduction Emphasizing Chemical Equilibria in Natural Waters*. Wiley-Interscience, New York, 1970, p. 583.
15. D. Thiry, L. Molina-Luna, E. Gautron, N. Stephant, A. Chauvin, K. Du, J. Ding, C. –H. Choi, P.-Y. Tessier and A. –A. El Mel, *Chem. Mater.*, 2015, **27**, 6374–6384.
16. A. Earnshaw and N. N. Greenwood, In *Chemistry of the Elements, 2nd ed.;* Butterworth-Heinemann, Oxford, 1997.
17. Y. -F. Han, F. Chen, Z. Zhong, K. Ramesh, L. Chen and E. Widjaja, *J. Phys. Chem. B,* 2006, **110**, 24450−24456.
18. V. Iablokov, K. Frey, O. Geszti and N. Kruse, *Catal. Lett*., 2010, **134**, 210−216.

19. W. Wang, G. McCool, N. Kapur, G. Yuan, B. Shan, M. Nguyen, U. M. Graham, B. H. Davis, G. Jacobs, K. Cho and X. Hao, *Science*, 2012, **337**, 832−835.
20. S. Fritsch, J. E. Post, S. L. Suib and A. Navrotsky, *Chem Mater*., 1998, **10**, 474-479.
21. B. M. Tebo, J. R. Bargar, B. G. Clement, Gregor J. Dick, K. J. Murray, D. Parker, R. Verity, S. M. Webb, *Annu. Rev. Earth Planet. Sci*., 2004. **32**, 287–328.
22. A. Byström and A. M. Byström, *Acta Cryst.*, 1950, **3**, 146-154.
23. E. P. Jeffrey, *Proc. Natl. Acad. Sci*., *USA*, 1999, **96**, 10134-10139.
24. D. R. Lide, In *Handbook of Chemistry and Physics*, *CRC Press, 72nd edn*, 1991–1992.
25. R. B. King, In *Encyclopedia of Inorganic Chemistry*, Wiley, New York, 1994.
26. C. N. R. Rao and B. Raveau, In *Transition Metal Oxides: Structure, Properties, and Synthesis of Ceramic Oxides*, 2nd edn, Wiley-VCH, New York, 1998.
27. J. Pike, J. Hanson, L. Zhang and S. –W. Chan, *Chem. Mater*., 2007, **19,** 5609-5616.
28. H. Chen, J. He, C. Zhang and H. He, *J. Phys. Chem. C*, 2007, **111**, 18033–18038.
29. A. K. Sinha, M. Pradhan and T. Pal, *J. Phys. Chem. C*, 2013, **117**, 23976–23986.
30. L. Que Jr. and W. B. Tolman, *Nature*, 2008, **455**, 333–340.
31. R. J. K. Taylor, M. Reid, J. Foot and S. A. Raw, *Acc. Chem. Res*., 2005, **38**, 851–869.
32. S. L. Brock, N. Duan, Z. R. Tian, O. Giraldo, H. Zhou and S. L. Suib, *Chem. Mater*., 1998, **10**, 2619–2628.
33. M. Amini, M. M. Najafpour, S. Nayeri, B. Pashaei and M. Bagherzadeh, *RSC Adv*., 2012, **2**, 3654–3657.
34. S. K. Ghosh, J. Kang, M. Inokuchi and N. Toshima, *Appl. Catal*., *A*, 2013, **464**, 225–232.
35. I. Djerdj, D. Acon, Z. Jaglîcić and M. Niederberger, *J. Phys. Chem. C*, 2007, **111**, 3614–3623.
36. P. Li, C. Nan, Z. Wei, J. Lu, Q. Peng and Y. Li, *Chem. Mater*., 2010, **22**, 4232–4236.

37. N. Birkner, S. Nayeri, B. Pashaei, M. M. Najafpour, W. H. Casey and A. Navrotsky, *Proc. Natl. Acad. Sci. U. S. A.*, 2013, **110,** 8801–8806.
38. H. Rahaman and S. K. Ghosh, *RSC Adv.*, 2016, **6**, 4531-4539.
39. A. Ramĭrez, P. Hillebrand, D. Stellmach, M. M. May, P. Bogdanoff and S. Fiechter, *J. Phys. Chem. C*, 2014, **118**, 14073–14081.
40. S. Yin, X. Wang, Z. Mou, Y. Wu, H. Huang, M. Zhu, Y. Du and P. Yang, *Phys. Chem. Chem. Phys.*, 2014, **16**, 11289–11296.
41. Z. Chen, Z. Jiao, D. Pan, Z. Li, M. Wu, C.-H. Shek, C. M. L. Wu and K. L. L. Joseph, *Chem. Rev.*, 2012, **112**, 3833–3855.
42. W. Weifeng, C. Xinwei, C. Weixing and G. I. Douglas, *Chem. Soc. Rev.*, 2011, **40**, 1697–1721.
43. G. S. Thomas, J. R. Bargar, S. Garrison and M. T. Bradley, *Acc. Chem. Res.*, 2010, **43**, 2–9.
44. . V. Polshettiwar, B. Baruwati and R. S. Varma, *ACS Nano*, 2009, **3**, 728–736.
45. M. Toupin, T. Brousse and D. Belanger, *Chem. Mater.*, 2002, **14**, 3946–3952.
46. C. N. Butterfield, A. V. Soldatova, S. –W. Lee, T. G. Spiro and B. M. Tebo, *Proc. Natl. Acad. Sci. USA.*, 2013, **110**, 11731–11735.
47. P. P. Sujith and P. A. Loka Bharathi, In *Progress in Molecular and Subcellular Biology*, 2011, 52, pp. 49−76.
48. C. R. Mayers and K. H. Nelson, *Science*, 1988, **240**, 1319−1321.
49. H. –P. Li, B. Daniel, D. Creeley, R. Grandbois, S. Zhang, C. Xu, Y. −Fang Ho, K. A. Schwehr, D. I. Kaplan, Peter H. Santschi, C. M. Hansel and C. M. Yeager, *Appl. Environ. Microbiol.*, 2014, 80, 2693−2699.
50. A. Fujishima and K. Honda, *Nature*, 1972, **238**, 37–40.
51. M. Grzelczak, J. Vermant, E. M. Furst and L. M. Liz-Marźan, *ACS Nano*, 2010, **4**, 3591–3605.
52. H. Cölfen and M. Antonietti, *Angew. Chem. Int. Ed.*, 2005, **44**, 5576–5591.
53. D. M. Vriezema, M. C. Aragones, J. A. A. W. Elemans, J. J. L. M. Cornelissen, A. E. Rowan and R. J. M. Nolte, *Chem. Rev.*, 2005, **105**, 1445–1489.
54. A. K. Sinha, M. Pradhan and T. Pal, *J. Phys. Chem. C*, 2013, **117**, 23976–23986.
55. S. K. Bikkarolla, F. Yu, W. Zhou, P. Joseph, P. Cumpson and P. Papakonstantinou, *J. Mater. Chem. A*, 2014, **2**, 14493–14501.
56. S. Yin, X. Wang, Z. Mou, Y. Wu, H. Huang, M. Zhu, Y. Du and P. Yang, *Phys. Chem. Chem. Phys.*, 2014, **16,** 11289–11296.

57. M. -Q. Yang, N. Zhang, M. Pagliaro and Y. -J. Xu, *Chem. Soc. Rev.*, 2014, **43**, 8240–8254.
58. G. S. Thomas, J. R. Bargar, S. Garrison and M. T. Bradley, *Acc. Chem. Res.*, 2010, **43,** 2-9.
59. V. Polshettiwar, B. Baruwati and R. S. Varma, *ACS Nano*, 2009, **3**, 728–736.
60. O. Giraldo, S. L. Brock, W. S. Willis, M. Marquez and S. L. Suib, *J. Am. Chem. Soc*., 2000, **122**, 9330–9331.
61. F. Y. Cheng, J. A. Shen, B. Peng, Y. D. Pan, Z. L. Tao and J. Chen, *Nat. Chem.*, 2011, **3**, 79–84.
62. H. M. Zang and Y. Teraoka, *Catal. Today*, 1989**, 6**, 155–162.
63. L. Hu, Q. Peng and Y. Li, *J. Am. Chem. Soc*., 2008, **130**, 16136–16137.
64. L. −C. Wang, X. −S. Huang, Q. Liu, Y. −M. Liu, Y. Cao, H. −Y. He, K. −N. Fan and J. −H. Zhuang, *J. Catal.*, 2008, **259**, 66−74.
65. M. Amini, M. M. Najafpour, S. Nayeri, B. Pashaei, M. Bagherzadeh, *Dalton Trans.*, 2012, **41**, 11026–11031.
66. W. Wei, X. Cui, W. Chena and D. G. Ivey, *Chem. Soc. Rev*., 2011, **40**, 1697–1721.
67. P. Simon and Y. Gogotsi, *Nat. Mater.*, 2008, **7,** 845–854.
68. P. J. Hall, M. Mirzaeian, S. I. Fletcher, F. B. Sillars, A. J. R. Rennie, G. O. Shitta-Bey, G. Wilson, A. Cruden and R. Carter, *Energy Environ. Sci.*, 2010, **3**, 1238–1251.
69. J. H. Alstrum-Acevedo, M. K. Brennaman and T. Meyer, *J. Inorg. Chem.*, 2005, **44**, 6802–6827.
70. F. Liu, J. J. Concepcion, J. W. Jurss, T. Cardolaccia, J. L. Templeton and T. Meyer, *J. Inorg. Chem.*, 2008, **47**, 1727–1752.
71. S. M. Barnett, K. I. Goldberg and J. M. Mayer, *Nature Chem.*, 2012, **4**, 498-502.
72. R. Eisenberg and H. B. Gray, *Inorg. Chem.*, 2008, **47**, 1697–1699.
73. Y. Tang and W. Cheng, *Langmuir*, 2013, **29**, 3125−3132.
74. J. P. McEvoy and G. W. Brudvig, *Chem. Rev.*, 2006, **106**, 4455–4483.
75. R. Ding, L. Qi, M. Jia and H. Wang, *Nanoscale*, 2014, **6**, 1369−1376.
76. S. Trassati In *Electrochemistry of Novel Materials*, J. Lipkowski and P. N. Ross, eds., Chapter 5, Wiley-VCH, Weinheim, 1994, pp. 207–296.
77. J. G. McAlpin, *J. Am. Chem. Soc.*, 2011, **133**, 15444–15452.

78. M. Wiechen, M. M. Najafpour, S. I. Allakhverdiev, and L. Spiccia, *Energy Environ. Sci.*, 2014, **7**, 2203–2212.
79. C. –H. Kuo, M. M. Islam, S. P. Altug, B. Sourav, A. M. El-Sawy, S. Wenqiao, Z. Luo, S. –Y. Chen, J. F. Rusling, H. Jie and S. L. Suib, *ACS Catal.*, 2015, **5**, 1693–1699.
80. C. E. Frey and K. Philipp, *Chem. Eur. J.*, 2015, **21**, 14958–14968.
81. M. M. Najafpour, R. Gernot, H. Małgorzata, N. M. Atefeh, E. –M. Aro, R. Carpentier, N. Hiroshi, J. E. –R. Julian, J. R. Shen and I. A. Suleyman, *Chem. Rev.*, 2016, **116**, 2886–2936.
82. R. J. K. Taylor, M. Reid, J. Foot and S. A. Raw, *Acc. Chem. Res*., 2005, **38**, 851–869.
83. J. Liu, J. Jiang, M. Bosman and J. F. Hong, *J. Mater. Chem.*, 2012, **22**, 2419–2426.
84. Y. Gorlin, F. J. Thomas, *J. Am. Chem. Soc.*, 2010, **132,** 13612–13614.
85. J. Huang, Z. Yang, Z. Feng, X. Xie and X. Wen, *Sci. Rep.*, 2016, **6**, 24471, 1−12.
86. S. Yu-Sheng and Z. Tian-Shu, *Sensors and Actuators B*, 1993, **12**, 5-9.
87. R. Hu, J. Wang, P. Chen, Y. Hao, C. Zhang and X. Li, *J. Nanomaterials*, 2014, 1-7.
88. V. V. Malyshev and A. V. Pislyakov, *J. Anal. Chem.*, 2014, **69**, 123–135.
89. F. Edelman, H. Hahn, S. Seifried, C. Alof, H. Hoche, A. Balogh , P. Werner, K. Zakrzewska, M. Radecka, P. Pasierb, A. Chack, V. Mikhelashvili, G. Eisenstein, *Mater. Sci. Eng. B*, 2000, **69–70**, 386–391.
90. A. K. Sinha, K. Suzuki, M. Takahara, H. Azuma, T. Nonaka, and K. Fukumoto, *Angew. Chem. Int. Ed.*, 2007, **46**, 2891–2894.
91. M.E. Franke, T. J. Koplin and U. Simon, *Small*, 2006, **2**, 36−50.
92. N. Gogurla, A. K. Sinha, S. Santra, S. Manna and S. K. Ray, *Sci. Rep.*, 2014, **4**, 6483 1−8.
93. X. Chu, X. Liu, and G. Meng, *Sens. Actuators B*, 1999, **55**, 19−22.
94. S.A. Majetich and Y. Jin, *Science*, 1999, **284**, 470–473.
95. A. R. Armstrong and P. G. Bruce, *Nature*, 1996, **381**, 499–500.
96. H. Rahaman and S. K. Ghosh, *RSC Adv.*, 2016, **6**, 4531-4539.
97. K. S. Shankar , S. Kar, G. N. Subbanna and A. K. Raychaudhuri, *Solid State Commun.*, 2004, **129**, 479–483.

98. K. Dwight and N. Menyuk, *Phys. Rev*., 1960, **119**, 1470–1479.
99. W. S. Seo, H. H. Jo, K. Lee, B. Kim, S. J. Oh and J. T. Park, *Angew. Chem. Int. Ed*., 2004, **43**, 1115–1115.
100. G. H. Lee, S. H. Huh, J. W. Jeong, B. J. Choi, S. H. Kim, H. -C. Ri, *J. Am. Chem. Soc*., 2002, **124**, 12094–12095.
101. W. S. Seo, H. H. Jo, K. Lee, B. Kim, S. J. Oh and J. T. Park, *Angew. Chem. Int. Ed*., 2004, **43**, 1115 –1115.
102. W. Yan, T. Ayvazian, J. Kim, Y. Liu, K. C. Donavan, W. Xing, Y. Yang, J. C. Hemminger and Reginald M. Penner, *ACS Nano*, 2011, **5**, 8275–8287.
103. K. H. Bae, K. Lee, C. Kim and T. G. Park, *Biomaterials*, 2011, **32,** 176−184.
104. E. –J. Kim, C. –S. Lee, Y. –Y. Chang and Y. –S. Chang, *ACS Appl. Mater. Interfaces*, 2013, **5**, 9628− 9634.
105. J. W. Long, L. R. Qadir, R. M. Stroud and D. R. Rolison, *J. Phys. Chem. B*, 2001, **105**, 8712−8717.